IVYSPRING INTERNATIONAL PUBLISHER

*Theranostics*

2017; 7(5): 1214-1224. doi: 10.7150/thno.17252

Research Paper

# Size-dependent Effects of Gold Nanoparticles on Osteogenic Differentiation of Human Periodontal Ligament Progenitor Cells

Yangheng Zhang[1], Na Kong[2], Yuanchao Zhang[2], Wenrong Yang[2], Fuhua Yan[1]✉

1. Nanjing Stomatological Hospital, Medical School of Nanjing University, Nanjing, Jiangsu, China;
2. School of Life and Environmental Science, Centre for Chemistry and Biotechnology, Deakin University, Geelong, Victoria 3216, Australia.

✉ Corresponding author: Fuhua Yan, 30 Zhongyang Road, Nanjing, Jiangsu, 210008, China. Tel: +86-25-83620253 Fax: +86-25-83620202 E-mail: yanfh@nju.edu.cn



Received: 2016.08.18; Accepted: 2017.01.24; Published: 2017.03.06

## Abstract

Gold nanoparticles (AuNPs) have been reported to promote osteogenic differentiation of mesenchymal stem cells and osteoblasts, but little is known about their effects on human periodontal ligament progenitor cells (PDLPs). In this study, we evaluated the effects of AuNPs with various diameters (5, 13 and 45 nm) on the osteogenic differentiation of PDLPs and explored the underlying mechanisms. 5 nm AuNPs reduced the alkaline phosphatase activity, mineralized nodule formation and expression of osteogenic genes, while 13 and 45 nm AuNPs increased these osteogenic markers. Compared with 13 nm, 45 nm AuNPs showed more effective in promoting osteogenic differentiation. Meanwhile, autophagy was up-regulated by 13 and 45 nm AuNPs but blocked by 5 nm AuNPs, which corresponded with their effects on osteogenic differentiation and indicated that autophagy might be involved in this process. Furthermore, the osteogenesis induced by 45 nm AuNPs could be reversed by autophagy inhibitors (3-methyladenine and chloroquine). These findings revealed that AuNPs affected the osteogenic differentiation of PDLPs in a size-dependent manner with autophagy as a potential explanation, which suggested AuNPs with defined size could be a promising material for periodontal bone regeneration.

Key words: gold nanoparticles; human periodontal ligament progenitor cells; osteogenic differentiation; autophagy; size-dependent.

## Introduction

Periodontitis, one of the most ubiquitous oral diseases, is a chronic inflammatory disease that destroys tooth-supporting tissues [1]. If left untreated, periodontitis can lead to progressive loss of the periodontal bone and subsequent tooth loss [2]. The ultimate goal of periodontal therapy is to achieve periodontal tissue regeneration, in which bone tissue regeneration is a crucial part [3]. The periodontal ligament (PDL) is located between teeth and alveolar bone and plays an integral role in the maintenance and regeneration of periodontal tissue. It was well documented that PDL contain a population of progenitor cells that retain the capacity to differentiation to different lineages [4]. Periodontal ligament progenitor cells (PDLPs), with stem-cell-like properties, exhibit great potential for repair periodontal tissue including the formation of new bone [5, 6]. Therefore, the development of effective strategies for promoting osteogenic differentiation of PDLPs has attracted particular attention in the field of periodontal regenerative.

Gold nanoparticles (AuNPs) have sparked increasing interests as promising nanomaterials in biological imaging, drug delivery, diagnosis and treatment of diseases, due to their unique optical properties, good biocompatibility, easy synthesis and functionalization [7, 8]. Recently, there is accumulating evidence that AuNPs can promote cell

osteogenic differentiation and mineralization. Gelatin-chitosan capped AuNPs [9] or self-assembled collagen AuNPs [10] could act as an efficient matrix for the growth of hydroxyapatite crystals. Yi et al. [11] showed that AuNPs facilitated the differentiation of bone marrow-derived mesenchymal stem cells (MSCs) towards osteoblast over adipocytes through activating the p38 MAPK signaling pathway. Choi et al. [12] depicted that AuNPs promoted osteogenesis of adipose-derived MSCs through the Wnt/β-catenin signaling pathway. Similarly, AuNPs also exerted a positive effect on osteogenic differentiation of osteoblasts [13, 14]. In a further vivo study, a AuNP-hydrogel complex was presented to enhance new bone formation at bone defect sites and these results were similar to those obtained with Gel-BMP [15]. These facts indicated that AuNPs might be potential candidates for therapy in bone tissue regeneration. Additionally, a recent pre-clinical study has shown that titanium dental implant surface coated with AuNPs can be useful as osteoinductive agents for formation of an osseous interface and promotion of bone regeneration [16].

Nanoparticles (NPs), including AuNPs, have been demonstrated as a novel class of autophagy modulators [17, 18]. Previous studies suggested that autophagy played an important role in the osteogenic differentiation of MSCs [19, 20] and osteoblasts [21-23]. Early induction of autophagy was required for osteogenic differentiation of human MSCs, and genetic or pharmacological autophagy inhibition all blocked osteogenetic process [20, 23]. Herein, we hypothesized that AuNPs could promote osteogenic differentiation of PDLPs to repair lost periodontal bone tissues and autophagy was involved in this process.

However, it's worth noting that the pro-osteogenic effects of AuNPs are depending on their properties, in particular the sizes of nanoparticles. Li et al. [24] compared the pro-osteogenic effects of 40, 70 and 110 nm AuNPs and found that 40 and 70 nm AuNPs were more effective. Similar results were obtained in another study, where the osteogenic effects of 30 and 50 nm AuNPs were superior to those of smaller (15nm) and bigger (75 and 100 nm) AuNPs [25]. In contrary, Zhang et al. [13] observed that the osteogenic effect of 20 nm AuNPs on primary osteoblasts was better than that of 40 nm AuNPs. This discrepancy in these results suggested that there was an urgent need to understand the osteogenic effects of AuNPs with various sizes.

This study aimed to investigate the effects of AuNPs on the osteogenic differentiation of PDLPs and compared the osteogenic effects of AuNPs with various sizes. Considering both the ability of AuNPs to induce autophagy and the important role of autophagy in osteogenic differentiation, we also further evaluated the role of autophagy in the process of AuNP-mediated osteogenic differentiation.

## Materials and Methods

### Gold nanoparticles synthesis and characterization

AuNPs with diameters of 5, 13 and 45 nm were synthesized from $HAuCl_4$ by chemical reduction method according to our previous report [26]. Briefly, for 5 nm AuNPs [27], 1 mL of 1 wt% $HAuCl_4 \cdot 3H_2O$ was added to 90 mL of deionized water. After 1 min of stirring, 2 mL of 38.8 mM sodium citrate was added and then stirred for another minute. 1 mL of fresh 0.075 wt% $NaBH_4$ in 38.8 mM sodium citrate was slowly added and stirred for another 5 min. As for the AuNPs with diameters of 13 and 45 nm [28], 1 mL of 5 mM $HAuCl_4 \cdot 3H_2O$ solution was added to 18 mL deionized water under stirring and heating until boiling. Then, 0.5% w/w sodium citrate as the reducing agent was added to reduce the $Au^{3+}$ to $Au^0$ by heating and stirring until the color change was evident. By varying the amount of sodium citrate (1 and 0.365 mL), AuNPs with 13 and 45 nm were synthesized, respectively. The final solution was topped up to 20 mL and the final concentration of the prepared gold colloid was approximately 0.25 mM. Then, 100 μL of 0.1 mM L-cysteine solution was added to 5 mL of freshly prepared AuNPs with 2 hours of stirring. The L-cysteine modified AuNPs were washed by centrifugation to remove unbound L-cysteine and dispersed in deionized water. All reagents mentioned above for AuNPs synthesis were purchased from Sigma-Aldrich. The quality and size properties of the synthesized AuNPs were examined under ultraviolet-visible (UV-Vis) spectrometer (CARY 300 Bio UV–Vis spectrometer), dynamic light scattering (DLS, Nano-ZS, Malvern Instrument) and transmission electron microscopy (TEM, JEOL-2100F, Japan).

### Cell culture

Human PDL cells were obtained from a commercial source (ScienCell research laboratories, CA, USA). PDL cells were isolated individually from impacted third molars or premolars extracted for orthodontic treatment from three healthy donors (two male, one female; age range 12-18 years) by enzyme digestion [4]. Briefly, periodontal ligament were gently scraped from the root surface and then digested in a solution of collagenase type I (3 mg/mL) and dispase (4 mg/mL) for 1 hour at 37°C. Cells were

dispersed into culture flasks and incubated in growth medium (DMEM supplemented with 1% penicillin/streptomycin and 10% fetal bovine serum) at 37 °C in 5% CO2. PDL cells were pooled and filtered through a 70 μm strainer. The single-cell suspensions were then plated in 100 mm culture dishes at low density ($1\times10^4$ cells/dish). Cells with colony-forming ability were harvested and used in subsequent experiments [29, 30]. Cells were used between passages 2 and 6.

For osteogenic induction, growth medium was replaced with osteogenic differentiation medium (growth medium supplemented with 0.1 μM dexamethasone, 50 μg/mL ascorbic acid, and 10 mM β-glycerophosphate). In the process of osteogenic differentiation, the culture medium was replaced every 3 days. In some of the differentiation experiments, autophagy inhibitors 3-methyladenine (3-MA, 2 mM) or chloroquine (CQ, 5 μM) was added to the culture.

### Cell viability assay

PDLPs viability was determined using Cell Counting Kit-8 (CCK-8; Dojindo Molecular Technologies, Tokyo, Japan). Cells were seeded into 96-well plates at the density of $5.0\times10^3$ cells/well and cultured in growth medium overnight. Then, AuNPs with the diameters of 5, 13 and 45 nm were added at the final concentrations of 0.1, 1 and 10 μM. After 48h of incubation, 10 μL of CCK-8 reagent was added into every well and incubated for 4h. The absorbance was measured by a SpectraMax M3 microplate reader (Molecular Devices, CA, USA) at a wavelength of 450 nm. Cell viability was expressed as a percentage relative to the control groups after subtraction of the background absorbance.

### Transmission electron microscopy

The uptake of AuNPs was examined using TEM (Tecnai G2 Spirit Biotwin, FEI Company, USA). PDLPs ($2.5\times10^5$ cells/well) were seeded into 6-well plates and cultured in growth medium overnight. Then the medium was replaced with osteogenic differentiation medium containing 5, 13 or 45 nm AuNPs at the concentration of 10 μM. After 3 days of incubation, the cells were fixed with 2.5% glutaraldehyde and subsequently in 1% osmium tetroxide, dehydrated in a graded series of ethanol and eventually embedded in epoxy resin. Ultrathin sections were examined with TEM at an accelerating voltage of 120 kV.

### Alkaline phosphatase activity and staining

ALP activity assay was performed using Alkaline Phosphatase Assay Kit (Abcam, MA, USA). PDLPs ($5.0\times10^4$ cells/well) were seeded into 24-well plates. After cultured in growth medium overnight, the cells were incubated with AuNPs (10 μM) with various size in osteogenic differentiation medium. On day 3 and 7, the cells were washed with PBS twice and lysed in the assay buffer, followed by centrifugation at $1.5\times10^4$ rpm to remove the insoluble substance. Then, 80 μL of the supernatant from each sample was added to 96-well plates and mixed with 50 μL of 5 mM pNPP solution. The plate was incubated at 25 °C for 60 min protected from light. The reaction with pNPP was stopped by adding 20 μL of stop solution. The absorbance was measured at 405 nm using a SpectraMax M3 microplate reader. A standard curve was performed, and the ALP activity level was expressed as a percentage relative to the control.

ALP staining was performed on day 7. The plates were washed with PBS and then fixed with 4% paraformaldehyde for 30 min. Then, the cells were stained using the BCIP/NBT alkaline phosphatase staining Kit (Beyotime Institute of Biotechnology, Shanghai, China) according to the manufacturer's instructions.

### Mineral deposition assay

Mineral deposition was examined by alizarin red S (ARS) and von Kossa staining. PDLPs were cultured and treated as described in the ALP activity assay. On day 21, cells were washed with PBS twice, fixed for 30 min using 4% paraformaldehyde. For ARS staining, cells were stained using 2% alizarin red S staining solution (Sigma-Aldrich) for 5 min. The unbound ARS were washed with water. For von Kossa staining, the fixed cells were washed with deionized water and incubated with 5% silver nitrate (Sigma-Aldrich) solution for 1 h under ultraviolet light, followed by treatment with 10% sodium thiosulphate (Sigma-Aldrich) for 5 min. As for both staining methods, the plates were examined using an inverted optical microscopy (Olympus IMT-2, Tokyo, Japan) and photographed using a digital camera (Canon EOS 70D, USA). ARS was quantified by measuring the absorbance at 562 nm after the stained cells were desorbed with 10% (w/v) cetylpyridinium chloride (Sigma-Aldrich). The von Kossa staining was quantified densitometrically with Image J.

### Real-time quantitative PCR

Real-time quantitative PCR was performed to evaluate the mRNA expression of osteogenic genes and autophagy genes. PDLPs ($2.5\times10^5$ cells/well) were seeded into 6-well plates and cultured in growth medium overnight. Then the medium was replaced with osteogenic differentiation medium containing AuNPs (10 μM) alone, or co-treatment with autophagy inhibitors. The total RNA was extracted

using TRNzol Reagent (Tiangen, Beijing, China). cDNA was prepared by reverse transcription (PrimeScript RT Reagent Kit; Takara Bio, Otsu, Japan) and amplified by real-time quantitative PCR with the primers shown in Table 1. Relative quantification was achieved using the comparative $2^{-\Delta\Delta Ct}$ method. All of the samples were run in triplicate and normalized to GAPDH.

**Table 1.** Primer sequences.

| Primer name | Forward primer sequence(5′-3′) | Reverse primer sequence(5′-3′) |
|---|---|---|
| Runx2 | GGAGTGGACGAGGCAAGAGTTT | AGCTTCTGTCTGTGCCTTCTGG |
| ALP | GACCCTTGACCCCCACAAT | GCTCGTACTGCATGTCCCCT |
| COL1 | AGAACAGCGTGGCCT | TCCGGTGTGACTCGT |
| OPN | CTGAACGCGCCTTCTGATTG | ACATCGGAATGCTCATTGCTCT |
| OCN | GGCAGCGAGGTAGTGAAGAG | GATGTGGTCAGCCAACTCGT |
| LC3 | GCCTTCTTCCTGCTGGTGAAC | AGCCGTCCTCGTCTTTCTCC |
| Beclin1 | CCAGGATGGTGTCTCTCGCA | CTGCGTCTGGGCATAACGCA |
| GAPDH | CGCTCTCTGCTCCTCCTGTT | CCATGGTGTCTGAGCGATGT |

### Western blot

Western blot was performed to evaluate the expression of osteogenic proteins and autophagy proteins. PDLPs were treated as described above for PCR assay. Cells were harvested and lysed in RIPA lysis buffer (Beyotime). Equal protein from each sample was fractionated by SDS-PAGE and transferred onto PVDF membranes (Millipore, Bedford, MA, USA). After blocking with 5% nonfat dry milk in TBS for 1 h at room temperature, the membranes were incubated with the primary antibody overnight at 4℃. The primary antibodies were purchased from Abcam (Runx2, ALP, COL1, OPN, and p62) and Cell Signaling Technology (LC3). β-actin was used as an internal control. After four washes with TBST, the membranes were incubated with anti-rabbit or anti-mouse secondary antibody for 1 h. The proteins were visualized using a Tanon-5200 chemiluminescent imaging system (Tanon, Shanghai, China).

### Statistical analysis

Data were expressed as the means ± standard deviation (SD). Significant differences were determined using Student's t-test or one-way ANOVA as appropriate. A 2-tailed $p<0.05$ was considered as statistically significant. All data were analyzed with SPSS20.0.

## Results

### Characterization of AuNPs

AuNPs with various sizes (5, 13 and 45 nm) were synthesized by chemical reduction method. Since the color of AuNPs solution is sensitive to the size of NPs, the three types of AuNPs solutions displayed diverse colors (Fig. 1A). Characterization of AuNPs was carried out via TEM, DLS and UV-Vis spectroscopy. The TEM images showed that the obtained AuNPs were approximately spherical and were well monodispersed (Fig. 1B). The sizes of AuNPs were confirmed by DLS, and the results indicated that the average sizes of AuNPs were 5, 13 and 45 nm, respectively (Fig. 1C). UV-vis absorption spectra of AuNPs showed an increasing absorption peaks with increasing size: that were, 515 nm, 518 nm and 530 nm for 5, 13 and 45 nm AuNPs, respectively (Fig. 1D). Zeta-potential of AuNPs by DLS were -20.5±1 mV for 5 nm AuNPs, -25.2±0.5 mV for 13 nm AuNPs and -26.0±0.3 mV for 45 nm AuNPs; all of the AuNPs displayed negative surface charges.

### Effects of AuNPs on PDLPs viability

After incubated with AuNPs of each size for 48 h, PDLPs showed little morphological change (Fig. 2A). The viability of PDLPs treated with AuNPs was tested by CCK-8 assays at 48 h (Fig. 2B). AuNPs of all three sizes exhibited no significant cytotoxicity to PDLPs at concentrations of 0.1, 1 and 10 μM. All AuNPs at concentration of 10 μM displayed a slightly positive effect on cell viability, and there was no significant difference among the three AuNP-treated groups. These results indicated that the AuNPs had good biocompatibility when the concentration was no higher than 10 μM. Therefore, the concentration of 10 μM was used in the following experiments.

### Uptake and localization of AuNPs in PDLPs

The uptake and intracellular localization of AuNPs were observed with TEM. TEM images (Fig. 2C) showed that AuNPs of all three sizes were internalized, most of them were found in intracellular vesicles. For 45 nm AuNPs, we observed one or two NPs clustered together. However, for 13 nm AuNPs, at least five NPs clustered together. The 5 nm AuNPs formed clusters of dozens of NPs. Generally, no AuNPs were observed in other cellular organelles, such as mitochondria, endoplasmic reticulum and nucleus.

All of the AuNP-treated groups displayed the accumulation of vesicles compared with control. Some of these vesicles were found to have a double membrane structure that is a typical feature of autophagosome. PDLPs treated with 13 and 45 nm AuNPs, rather than 5 nm, showed an increase in the number of autolysosomes, which result from the fusion of autophagosome with lysosome.

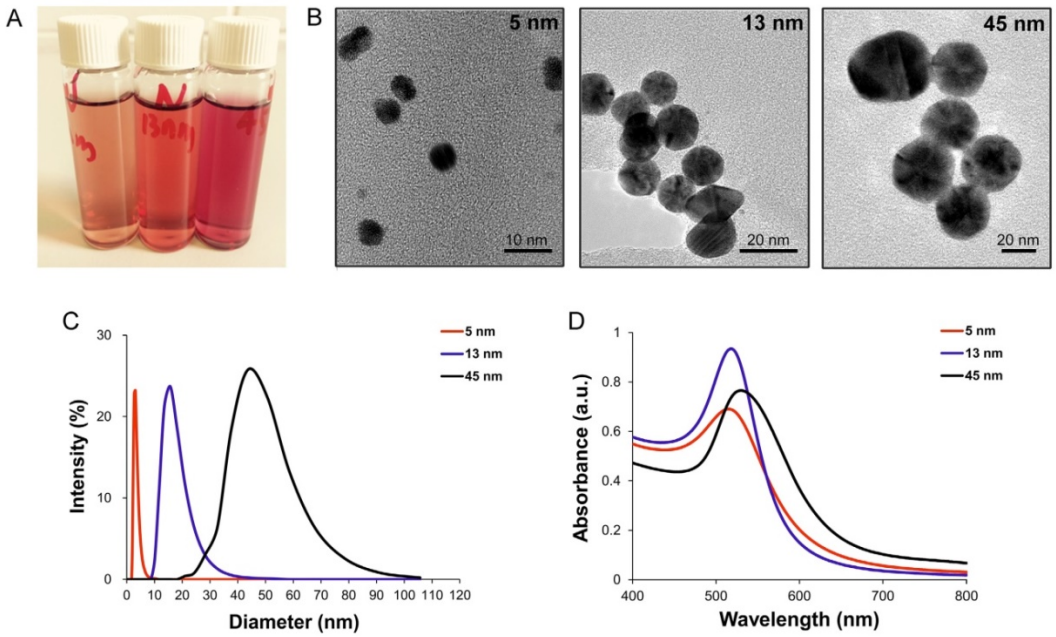


**Figure 1.** Characterization of AuNPs. (A) photographs (from left to right: 5, 13 and 45 nm), (B) TEM images, (C) size distribution, measured by DLS and (D) UV-vis absorption spectra of AuNPs with different sizes.

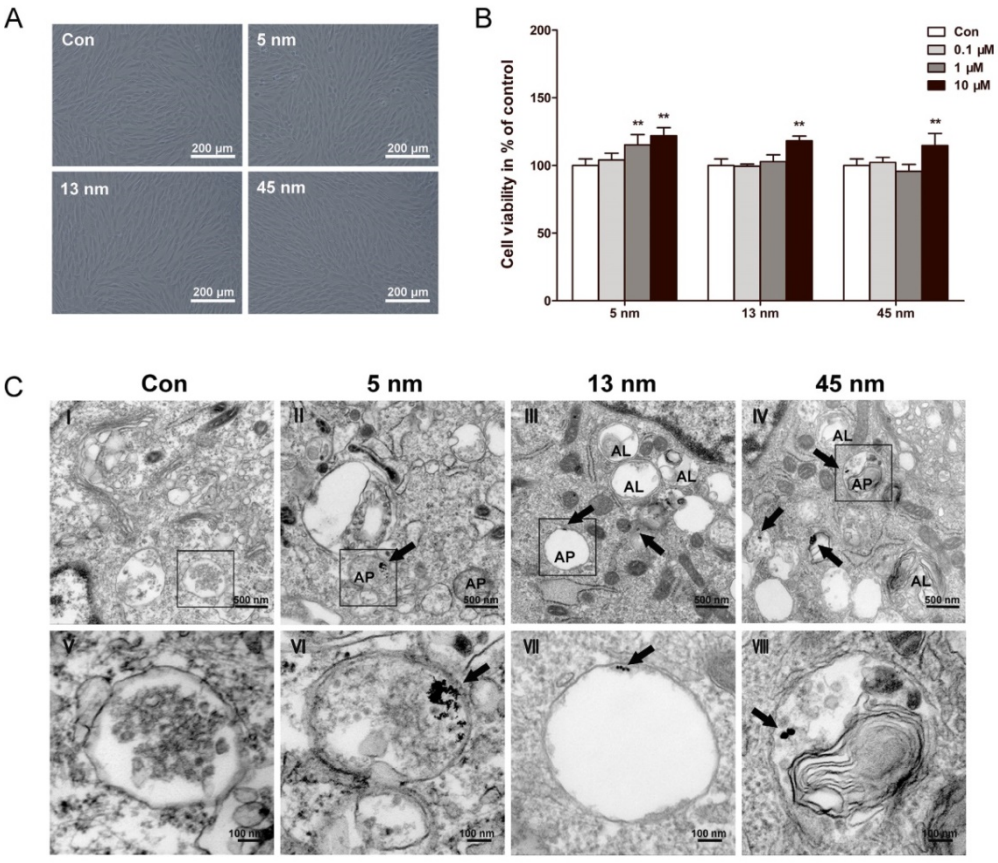


**Figure 2.** Biocompatibility and cellular uptake of AuNPs. PDLPs were treated with AuNPs with the diameters of 5, 13 and 45 nm, respectively. (A) Light microscope images of PDLPs treated with AuNPs (10 μM) for 48 h. (B) Effects of AuNPs on the viability of PDLPs were measured using CCK-8 at 48 h. $^{**}p<0.01$. (C) TEM images of PDLPs treated with AuNPs (10 μM) for 3 days. (V-VIII) were the high magnification images of the indicated portion in (I-IV), respectively. Arrows indicate internalized AuNPs, the labels "AP" indicate autophagosome, and the labels "AL" indicate autolysosome.

### Effects of AuNPs on ALP activity and mineralization

The effects of AuNPs on ALP activity were tested using ALP activity assay and ALP staining. On day 3 and 7, 5 nm AuNPs inhibited the ALP activity level, while 13 and 45 nm AuNPs raised ALP activity. 45 nm AuNPs exerted a more significant effect in increasing the ALP activity than 13 nm AuNPs (Fig. 3A). ALP staining on day 7 revealed the same tendency with ALP activity assay (Fig. 3B).

The effects of AuNPs on the formation of mineralized nodules were tested by ARS and von Kossa staining on day 21. As shown in Figure 3C, 5 nm AuNPs inhibited mineralization, whereas PDLPs treated with 13 and 45 nm AuNPs showed enhanced mineralized nodule formation. Mineral deposition of PDLPs cultured with 45 nm AuNPs was significantly higher than that of 13 nm AuNPs.

### Osteogenic gene expression

The effects of AuNPs on runt-related transcription factor 2 (Runx2), ALP, collagen type 1 (COL1), osteopontin (OPN) and osteocalcin (OCN) mRNA expression levels were determined by real-time PCR in PDLPs treated with AuNPs for 3, 5 and 7 days. As shown in Figure 4A, 5 nm AuNPs inhibited mRNA expression of these osteogenic genes at all time points, while 13 and 45 nm AuNPs accelerated their mRNA expression level. For 13 and 45 nm AuNP-treated groups, the expression of Runx2 and ALP rose from day 3, and the expression of COL1 and OPN started to increase on day 5. At each time point, 45 nm AuNPs had higher expression levels of these osteogenic genes than 13 nm AuNPs. Based on the results for mRNA expression, Runx2, ALP, COL1, and OPN were further analyzed on day 7 by western blot. As shown in Figure 4B, the protein expression levels were in agreement with the mRNA results. In particular, 5 nm AuNPs inhibited the expression of COL1 and OPN, while 13 and 45 nm AuNPs up-regulated all four osteogenic markers.

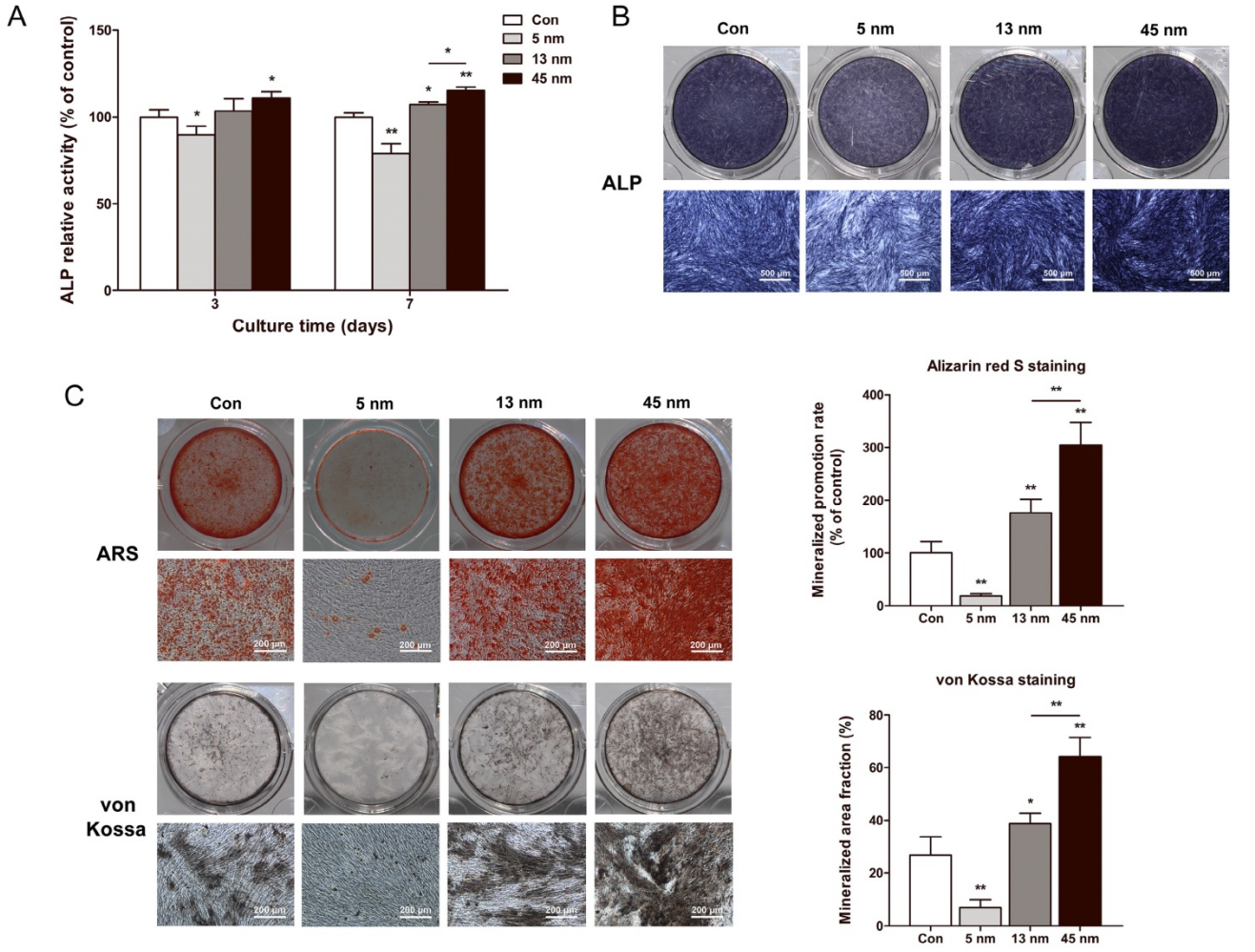


**Figure 3.** Effects of AuNPs on the ALP activity and mineralization. PDLPs were treated with AuNPs (5, 13 and 45 nm) at concentration of 10 μM. (A) ALP activity levels on day 3 and 7, (B) ALP staining on day 7, and (C) mineralized nodules stained with alizarin red S and von Kossa on day 21. *$p$<0.05, **$p$<0.01.

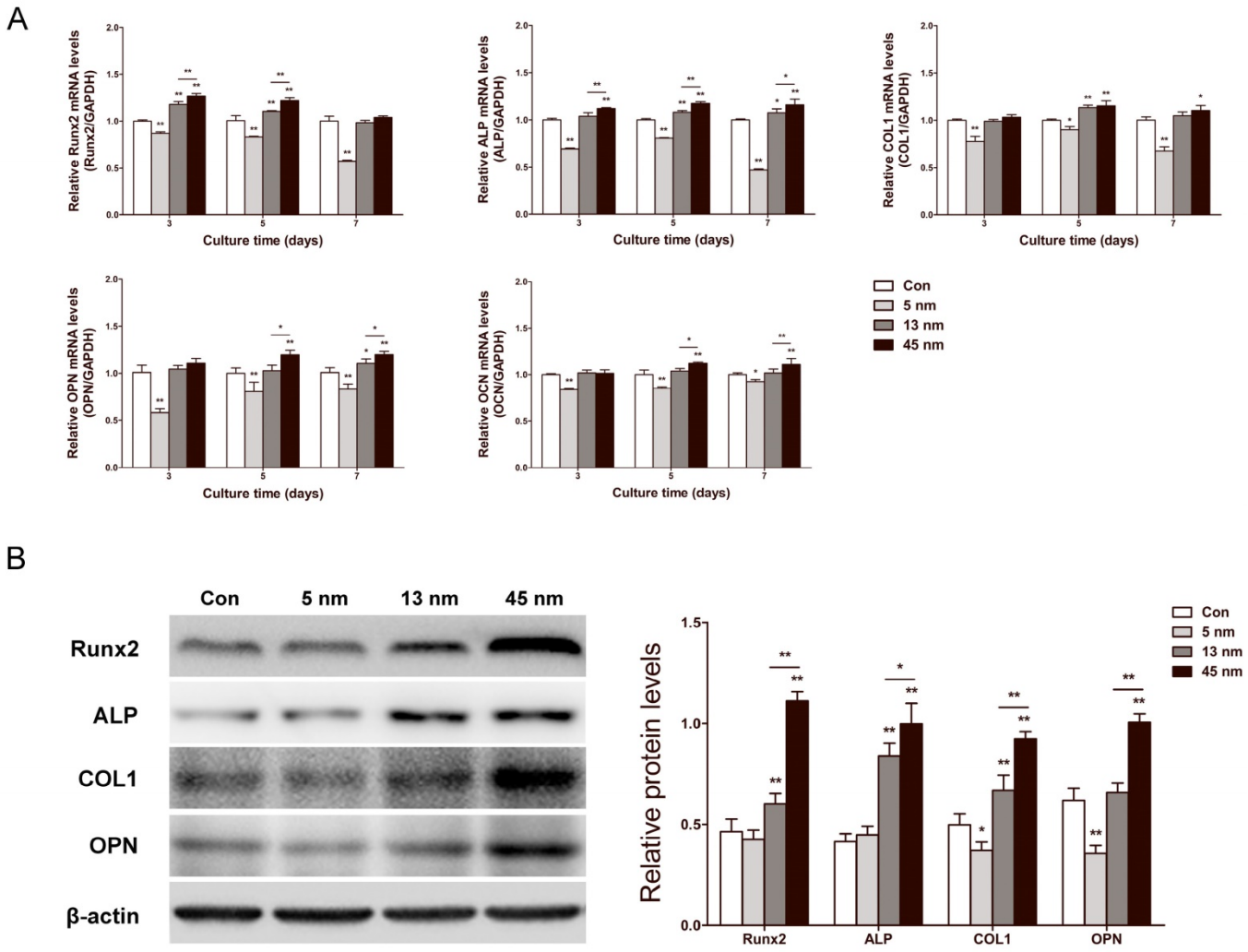


**Figure 4.** Effects of AuNPs on osteogenic gene expression. PDLPs were treated with AuNPs (5, 13 and 45 nm) at concentration of 10 μM. (A) Real-time PCR analysis of Runx2, ALP, COL1, OPN, and OCN mRNA expression on day 3, 5 and 7. (B) Western blot analysis of Runx2, ALP, COL1 and OPN protein expression on day 7. *$p$<0.05, **$p$<0.01.

## Effects of AuNPs on autophagy

To evaluate the change of autophagy in PDLPs treated with AuNPs, the expression of autophagy genes microtubule-associated protein light chain 3 (LC3) and Beclin1 were examined. On day 1 and 3, 13 and 45 nm AuNPs displayed a positive effect on the mRNA expression of LC3 and Beclin1, while 5 nm AuNPs inhibited their expression (Fig. 5A). Specifically, 45 nm AuNPs were more effective in up-regulating autophagy gene expression than 13 nm AuNPs. Western blots of LC3 and p62 were further analyzed on day 3 (Fig. 5B). The expression of LC3-II increased in all of the AuNP-treated groups in the following order, from the greatest increase to the lowest increase: 5, 45 and 13 nm. Meanwhile, the expression of p62 was reduced in 13 and 45 nm AuNPs groups but increased in 5 nm group.

## Effects of autophagy inhibition on 45 nm AuNP-induced osteogenesis

The involvement of autophagy in osteogenic differentiation induced by AuNPs was validated by autophagy inhibitors, 3-MA and CQ. Osteogenic differentiation of PDLPs was evaluated by ALP, ARS and von Kossa staining. The enhanced ALP activity and mineralization induced by 45 nm AuNPs were significantly decreased in the presence of autophagy inhibitors (Fig. 6A). Real-time PCR (Fig. 6B) and western blots (Fig. 6C) showed that the facilitation effects of 45 nm AuNPs on osteogenic genes expression (Runx2, ALP, COL1, OPN, OCN) were reversed by treatment with 3-MA or CQ.

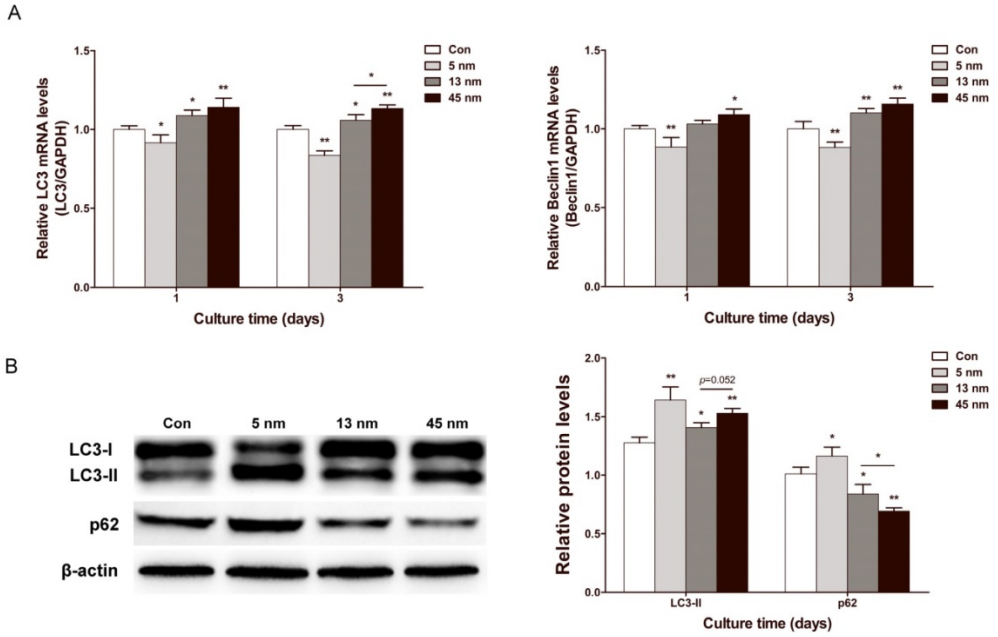


**Figure 5.** Effects of AuNPs on autophagy. PDLPs were treated with AuNPs (5, 13 and 45 nm) at concentration of 10 μM. (A) Real-time PCR analysis of LC3 and Beclin1 mRNA expression on day 1 and 3. (B) Western blot analysis of LC3-II and p62 expression on day 3. *$p$<0.05, **$p$<0.01.

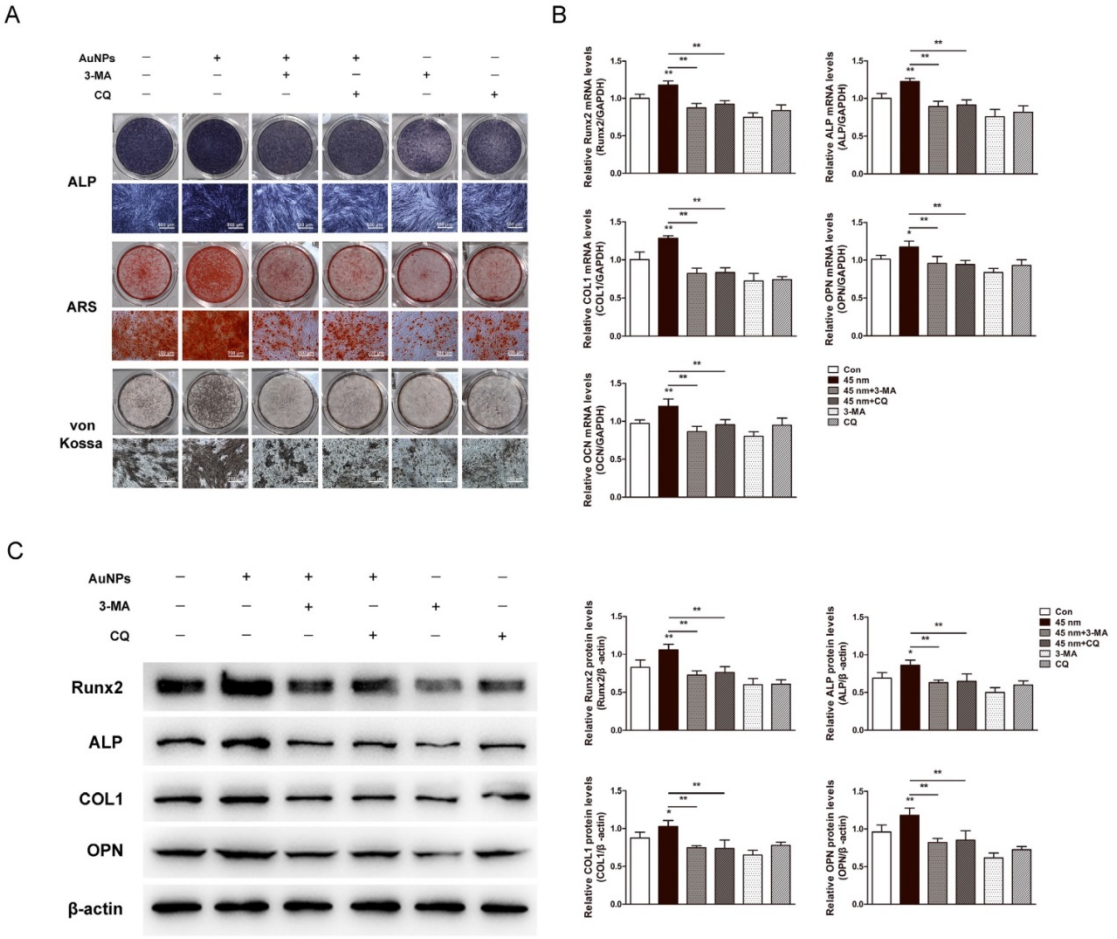


**Figure 6**. Effects of autophagy inhibitors on the 45 nm AuNP-induced osteogenic differentiation. PDLPs were treated with 45 nm AuNPs (10 μM) alone, or combine with 3-MA (2 mM) or CQ (5 μM). (A) ALP staining on day 7, alizarin red S and von Kossa staining on day 21. (B) Real-time PCR analysis of Runx2, ALP, COL1, OPN, and OCN mRNA expression on day 5. (C) Western blot analysis of Runx2, ALP, COL1 and OPN protein expression on day 7. *P* values for the comparison with control were selectively shown. *$p$<0.05, **$p$<0.01.

## Discussion

PDL contains a mixture of stem/progenitor cell populations at various stages of development that maintain homoeostasis and regeneration of periodontal tissue. To promote their osteogenic differentiation, there are several emerging approaches [31-33], among which AuNPs might be a promising material for periodontal bone regeneration. We observed whether AuNPs could promote osteogenic differentiation of PDLPs and compared the osteogenic effects of AuNPs with three different sizes. Our results indicated that AuNPs promoted osteogenic differentiation in a size-dependent manner, and AuNPs with the diameter of 45 nm have the optimal osteogenic effect among the three types of AuNPs.

To evaluate the biotoxicity of AuNPs, the viability of PDLPs incubated with 5, 13 and 45 nm AuNPs was analyzed. The results showed that AuNPs were non-toxic to PDLPs in the concentration range from 0.1 to 10 μM. We observed that all three types of AuNPs, in agreement with previous reports, displayed a slight positive effect on the viability of PDLPs [11, 13, 25]. This viability-promoting effect might be attributed to a nonspecific ROS-associated mechanism that can be induced by AuNPs [18, 34].

Based on the cell viability results, the effects of AuNPs on the osteogenic differentiation of PDLPs were assessed at a concentration of 10 μM. ALP activity serves as an early phenotypic marker, and mineralized nodule formation represents the final stages of osteogenic differentiation [35]. In our study, ALP activity and mineralization rate were higher in 13 and 45 nm AuNP groups, while 5 nm AuNPs obviously reduced ALP activity and mineralization of PDLPs. The expression of osteogenic genes was further assessed at both the mRNA and the protein levels. The results showed that the expression of genes was up-regulated by 13 and 45 nm AuNPs but down-regulated by 5 nm AuNPs, which matched the ALP activity and mineralized nodule formation results. During the process of osteogenic differentiation, the osteogenic genes are expressed at different stages. Runx2 is widely accepted as a key transcription factor for the initiation of osteogenesis that induces the expression of other genes, such as ALP and COL1 at an early stage and OPN and OCN at a late stage [36, 37]. Therefore, the influences of AuNPs on Runx2 and ALP started earlier. OPN was reported as a negative regulator for osteoblast precursor [38], its expression would be lower at the early stage of osteogenesis, but start to increase afterward. In this study, we found the OPN mRNA expression in 45 nm AuNPs treatment groups on day 3 was higher than the control without statistical significance, then elevated on day 5 and 7, which is consistent with previous reports [38]. This rapid up-regulation might allow OPN to become a negative feedback regulator for osteogenic differentiation.

Notably, 45 nm AuNPs were more potent than 13 nm AuNPs in accelerating the osteogenic differentiation of PDLPs. These results were in agreement with the previous study, where Ko et al. [25] reported that 30 and 50 nm AuNPs have greater osteogenic effects than 15 nm AuNPs. Unexpectedly, 5 nm AuNPs were observed to inhibit the osteogenic differentiation of PDLPs in the present study. As far as we know, there is no evidence regarding the osteogenic effects of AuNPs smaller than 10 nm. Taken together, these data confirm that size is a critical factor of AuNPs for promoting osteogenic differentiation.

Cellular uptake plays a vital role in the cellular response to AuNPs [39]. It has been reported that AuNPs of 40-50 nm resulted in optimal cellular uptake efficiency [40]. In this study, the uptake and intracellular localization of AuNPs with different sizes were also observed. AuNPs of the three sizes were all internalized into intracellular vesicles. The cellular uptake of AuNPs was affected by thermodynamic driving force [40]. AuNPs smaller than 50 nm cannot produce enough free energy to enter cells and thus must cluster together to create enough driving force for uptake. In the TEM images, we observed that 5 nm AuNPs clustered together, with dozens of NPs in the clusters, while 13 and 45 nm AuNPs clustered together much less. Meanwhile, autophagosomes and autolysosomes were also observed in AuNP-treated groups, implying that AuNPs were able to induce autophagy.

NPs, such as AuNPs, bioactive silica NPs and titanium dioxide NPs, have been regarded as a novel class of autophagy activator [17, 18, 41, 42]. Autophagy is a lysosome-based degradative pathway that plays an important role in various physiological and pathological events, including osteogenic differentiation [19, 23, 43]. A recent study confirmed that bioactive silica NPs could increase osteoblast differentiation via stimulation of autophagy [41]. Our TEM images also indicated that PDLPs treated with AuNPs contained more autophagic vesicles. Therefore, autophagy is probably involved in the response of PDLPs to AuNPs, affecting the osteogenic process. To test this hypothesis, we examined the expression of representative genes involved in the autophagy pathway [44]. The mRNA expression of LC3 and Beclin1 was up-regulated by 13 and 45 nm AuNPs but down-regulated by 5 nm AuNPs. We further monitored the induction of autophagy by AuNPs at the protein level. All of the AuNPs enhanced the expression of LC3-II, which is indicative

of autophagosome formation [44]. However, 5 nm AuNPs induced the highest increase in the expression of LC3-II, which was not consistent with mRNA expression. One possible explanation is that excessive accumulation of autophagosomes leads to suppression of LC3 mRNA expression. This explanation was further supported by the expression level of p62. The accumulation of autophagosomes can result from true induction of autophagy or blockade of autophagic flux (the turnover of autophagosomes by lysosomes) [45, 46]. p62, a substrate that is preferentially degraded by autophagy, can be used to monitor autophagic flux [45]. Our results showed that the degradation of p62 was blocked in PDLPs treated with 5 nm AuNPs, which indicated that autophagosomes accumulation in this group resulted from blockade of autophagic flux [46]. Taken together, our findings suggest that treatment with 13 and 45 nm AuNPs resulted in true induction of autophagy, while 5 nm AuNPs did not. This phenomenon corresponded to the pro-osteogenic effects of AuNPs with various sizes.

To further investigate whether the osteogenic differentiation induced by AuNPs depend on autophagy activation, we utilized inhibitors of different stages of autophagy (3-MA and CQ). The 45 nm AuNPs were chosen since they exhibited the best pro-osteogenic effect among the three sizes. 3-MA blocks the formation of autophagosome by inhibiting the class III phosphatidylinositol 3-kinase, and CQ inhibits autophagy at a later step by blocking the degradation of autolysosome [45, 47]. Both 3-MA and CQ significantly reversed the osteogenesis enhanced by 45 nm AuNPs, suggesting the pro-osteogenic effect of 45 nm AuNPs was related to the activation of autophagy, which is consistent with the previous studies [19-23]. Pantovic et al. [20] reported that the RNA interference-mediated silencing of autophagy-essential LC3β, as well as the pharmacological inhibitors of autophagy, each suppressed mesenchymal stem cell differentiation to osteoblasts. Nollet et al. [21] showed that knockdown of autophagy-related gene (Atg) 7 or Beclin1 with siRNAs induced a significant decrease in mineralization of osteoblasts, and the deletion of Atg5 resulted in decreased bone formation *in vivo*. In another study, the deletion of an essential component of the autophagosome complex (FIP 200) led to deficient autophagy, bone formation and mineralization [23]. These evidences implied that autophagy might be an underlying mechanism for AuNP-mediated osteogenic differentiation.

There are still some limitations in present study. Firstly, this study showed that AuNPs affected osteogenesis in a size-dependent manner. This size effects should be further validated *in vivo*. Secondly, pharmacological autophagy inhibition might be not stable and complete, which calls for genetic modification related to autophagy. Thirdly, the study only suggested a potential connection between autophagy and osteogenic differentiation. How they interact need be thoroughly and carefully explored to get a comprehensive understanding of the role of autophagy in AuNP-mediated osteogenesis.

## Conclusions

This study is the first report of the size-dependent effects of AuNPs on the osteogenic differentiation of PDLPs, in which 45 nm AuNPs showed the highest potency to promote osteogenesis. The results also suggested a probable connection between autophagy and the observed osteogenic effects. Actually AuNPs with various sizes acted differently on autophagy, which provided a potential explanation for why different AuNPs showed different potencies for osteogenesis. These findings help to provide a new perspective for the role of autophagy in AuNP-mediated osteogenic differentiation and suggest that AuNPs are potential candidates for periodontal regeneration therapy and bone tissue engineering.

## Abbreviations

AuNPs: Gold nanoparticles; PDLPs: periodontal ligament progenitor cells; PDL: periodontal ligament; MSCs: mesenchymal stem cells; UV-Vis: ultraviolet-visible; DLS: dynamic light scattering; TEM: transmission electron microscopy; 3-MA: 3-methyladenine; CQ: chloroquine; CCK-8: Cell Counting Kit-8; ALP: alkaline phosphatase activity; ARS: alizarin red S; NPs: nanoparticles; Runx2: runt-related transcription factor 2; COL1: collagen type 1; OPN: osteopontin; OCN: osteocalcin; LC3: microtubule-associated protein light chain 3; Atg: autophagy-related gene.

## Acknowledgements

This study was supported by the National Natural Science Foundation Project (No. 81570982), the "Six Talent Peaks" of High Level Talent Selection and Training Project of Jiangsu Province (No. 2013-SWYY-006), the Double Innovation Talent Introduction Plan of Jiangsu Province (No.su rencai ban[2014]27), and the International Cooperation Research and Develop Project of Nanjing Health Bureau (No. 201605083).

## Competing Interests

The authors have declared that no competing interest exists.

## References


1. Pihlstrom BL, Michalowicz BS, Johnson NW. Periodontal diseases. Lancet. 2005; 366: 1809-20.
2. Khan SA, Kong EF, Meiller TF, Jabra-Rizk MA. Periodontal Diseases: Bug Induced, Host Promoted. PLoS Pathog. 2015; 11(7): e1004952.
3. Larsson L, Decker AM, Nibali L, Pilipchuk SP, Berglundh T, Giannobile WV. Regenerative Medicine for Periodontal and Peri-implant Diseases. J Dent Res. 2016; 95: 255-66.
4. Seo BM, Miura M, Gronthos S, Bartold PM, Batouli S, Brahim J, et al. Investigation of multipotent postnatal stem cells from human periodontal ligament. Lancet. 2004; 364: 149-55.
5. Nagatomo K, Komaki M, Sekiya I, Sakaguchi Y, Noguchi K, Oda S, et al. Stem cell properties of human periodontal ligament cells. J Periodontal Res. 2006; 41: 303-10.
6. Bartold PM, Shi S, Gronthos S. Stem cells and periodontal regeneration. Periodontol 2000. 2006; 40: 164-72.
7. Boisselier E, Astruc D. Gold nanoparticles in nanomedicine: preparations, imaging, diagnostics, therapies and toxicity. Chem Soc Rev. 2009; 38: 1759-82.
8. Khlebtsov N, Bogatyrev V, Dykman L, Khlebtsov B, Staroverov S, Shirokov A, et al. Analytical and Theranostic Applications of Gold Nanoparticles and Multifunctional Nanocomposites. Theranostics. 2013; 3: 167-80.
9. Sobhana SSL, Sundaraseelan J, Sekar S, Sastry TP, Mandal AB. Gelatin-Chitosan composite capped gold nanoparticles: a matrix for the growth of hydroxyapatite. J Nanopart Res. 2009; 11: 333-40.
10. Aryal S, Bahadur K. C R, Bhattarai SR, Prabu P, Kim HY. Immobilization of collagen on gold nanoparticles: preparation, characterization, and hydroxyapatite growth. J Mater Chem. 2006; 16: 4642-8.
11. Yi C, Liu D, Fong CC, Zhang J, Yang M. Gold Nanoparticles Promote Osteogenic Differentiation of Mesenchymal Stem Cells through p38 MAPK Pathway. ACS Nano. 2010; 4: 6439-48.
12. Choi SY, Song MS, Ryu PD, Lam AT, Joo SW, Lee SY. Gold nanoparticles promote osteogenic differentiation in human adipose-derived mesenchymal stem cells through the Wnt/beta-catenin signaling pathway. Int J Nanomedicine. 2015; 10: 4383-92.
13. Zhang D, Liu D, Zhang J, Fong C, Yang M. Gold nanoparticles stimulate differentiation and mineralization of primary osteoblasts through the ERK/MAPK signaling pathway. Mater Sci Eng C Mater Biol Appl. 2014; 42: 70-7.
14. Yao Y, Shi X, Chen F. The Effect of Gold Nanoparticles on the Proliferation and Differentiation of Murine Osteoblast: A Study of MC3T3-E1 Cells In Vitro. J Nanosci Nanotechnol. 2014; 14: 4851-7.
15. Heo DN, Ko WK, Bae MS, Lee JB, Lee D-W, Byun W, et al. Enhanced bone regeneration with a gold nanoparticle-hydrogel complex. J Mater Chem B Mater Biol Med. 2014; 2: 1584-93.
16. Heo DN, Ko WK, Lee HR, Lee SJ, Lee D, Um SH, et al. Titanium dental implants surface-immobilized with gold nanoparticles as osteoinductive agents for rapid osseointegration. J Colloid Interface Sci. 2016; 469: 129-37.
17. Zabirnyk O, Yezhelyev M, Seleverstov O. Nanoparticles as a novel class of autophagy activators. Autophagy. 2007; 3: 278-81.
18. Li JJ, Hartono D, Ong CN, Bay BH, Yung LY. Autophagy and oxidative stress associated with gold nanoparticles. Biomaterials. 2010; 31: 5996-6003.
19. Li Y, Guo T, Zhang Z, Yao Y, Chang S, Nor JE, et al. Autophagy Modulates Cell Mineralization on Fluorapatite-Modified Scaffolds. J Dent Res. 2016; 95: 650-6.
20. Pantovic A, Krstic A, Janjetovic K, Kocic J, Harhaji-Trajkovic L, Bugarski D, et al. Coordinated time-dependent modulation of AMPK/Akt/mTOR signaling and autophagy controls osteogenic differentiation of human mesenchymal stem cells. Bone. 2013; 52: 524-31.
21. Nollet M, Santucci-Darmanin S, Breuil V, Al-Sahlanee R, Cros C, Topi M, et al. Autophagy in osteoblasts is involved in mineralization and bone homeostasis. Autophagy. 2014; 10: 1965-77.
22. Kaluderovic MR, Mojic M, Schreckenbach JP, Maksimovic-Ivanic D, Graf H-L, Mijatovic S. A Key Role of Autophagy in Osteoblast Differentiation on Titanium-Based Dental Implants. Cells Tissues Organs. 2014; 200: 265-77.
23. Liu F, Fang F, Yuan H, Yang D, Chen Y, Williams L, et al. Suppression of Autophagy by FIP200 Deletion Leads to Osteopenia in Mice Through the Inhibition of Osteoblast Terminal Differentiation. J Bone Miner Res. 2013; 28: 2414-30.
24. Li J, Li JJ, Zhang J, Wang X, Kawazoe N, Chen G. Gold nanoparticle size and shape influence on osteogenesis of mesenchymal stem cells. Nanoscale. 2016; 8: 7992-8007.
25. Ko WK, Heo DN, Moon HJ, Lee SJ, Bae MS, Lee JB, et al. The effect of gold nanoparticle size on osteogenic differentiation of adipose-derived stem cells. J Colloid Interface Sci. 2015; 438: 68-76.
26. Zhang Y, Liu J, Li D, Dai X, Yan F, Conlan XA, et al. Self-Assembled Core-Satellite Gold Nanoparticle Networks for Ultrasensitive Detection of Chiral Molecules by Recognition Tunneling Current. ACS Nano. 2016; 10: 5096-103.
27. Haiss W, Thanh NT, Aveyard J, Fernig DG. Determination of size and concentration of gold nanoparticles from UV-Vis spectra. Anal Chem. 2007; 79: 4215-21.
28. Weng Z, Wang H, Vongsvivut J, Li R, Glushenkov AM, He J, et al. Self-assembly of core-satellite gold nanoparticles for colorimetric detection of copper ions. Anal Chim Acta. 2013; 803: 128-34.
29. Zhou Q, Yang P, Li X, Liu H, Ge S. Bioactivity of periodontal ligament stem cells on sodium titanate coated with graphene oxide. Sci Rep. 2016; 6: 19343.
30. Dangaria SJ, Ito Y, Luan X, Diekwisch TG. Successful Periodontal Ligament Regeneration by Periodontal Progenitor Preseeding on Natural Tooth Root Surfaces. Stem Cells Dev. 2011; 20: 1659-68.
31. Inanc B, Elcin AE, Elcin YM. Osteogenic induction of human periodontal ligament fibroblasts under two- and three-dimensional culture conditions. Tissue Eng. 2006; 12: 257-66.
32. Inanc B, Eser Elçin A, Koc A, Balos K, Parlar A, Murat Elçin Y. Encapsulation and osteoinduction of human periodontal ligament fibroblasts in chitosan-hydroxyapatite microspheres. J Biomed Mater Res A. 2007; 82: 917-26.
33. Wu C, Zhou Y, Lin C, Chang J, Xiao Y. Strontium-containing mesoporous bioactive glass scaffolds with improved osteogenic/cementogenic differentiation of periodontal ligament cells for periodontal tissue engineering. Acta Biomater. 2012; 8: 3805-15.
34. Wedgwood S, Dettman RW, Black SM. ET-1 stimulates pulmonary arterial smooth muscle cell proliferation via induction of reactive oxygen species. Am J Physiol Lung Cell Mol Physiol. 2001; 281: L1058-L67.
35. Ravichandran R, Venugopal JR, Sundarrajan S, Mukherjee S, Ramakrishna S. Precipitation of nanohydroxyapatite on PLIA/PBLG/Collagen nanofibrous structures for the differentiation of adipose derived stem cells to osteogenic lineage. Biomaterials. 2012; 33: 846-55.
36. Komori T. Regulation of bone development and extracellular matrix protein genes by RUNX2. Cell Tissue Res. 2010; 339: 189-95.
37. Patil S, Paul S. A Comprehensive Review on the Role of Various Materials in the Osteogenic Differentiation of Mesenchymal Stem Cells with a Special Focus on the Association of Heat Shock Proteins and Nanoparticles. Cells Tissues Organs. 2014; 199: 81-102.
38. Huang W, Carlsen B, Rudkin G, Berry M, Ishida K, Yamaguchi DT, et al. Osteopontin is a negative regulator of proliferation and differentiation in MC3T3-E1 pre-osteoblastic cells. Bone. 2004; 34: 799-808.
39. Alkilany AM, Murphy CJ. Toxicity and cellular uptake of gold nanoparticles: what we have learned so far? J Nanopart Res. 2010; 12: 2313-33.
40. Chithrani BD, Chan WCW. Elucidating the mechanism of cellular uptake and removal of protein-coated gold nanoparticles of different sizes and shapes. Nano Lett. 2007; 7: 1542-50.
41. Ha S-W, Weitzmann MN, Beck GR, Jr. Bioactive Silica Nanoparticles Promote Osteoblast Differentiation through Stimulation of Autophagy and Direct Association with LC3 and p62. ACS Nano. 2014; 8: 5898-910.
42. Zhao Y, Howe JL, Yu Z, Leong DT, Chu JJ, Loo JS, et al. Exposure to Titanium Dioxide Nanoparticles Induces Autophagy in Primary Human Keratinocytes. Small. 2013; 9: 387-92.
43. Mizushima N, Levine B. Autophagy in mammalian development and differentiation. Nat Cell Biol. 2010; 12: 823-30.
44. Pyo JO, Nah J, Jung YK. Molecules and their functions in autophagy. Exp Mol Med. 2012; 44: 73-80.
45. Mizushima N, Yoshimori T, Levine B. Methods in Mammalian Autophagy Research. Cell. 2010; 140: 313-26.
46. Ma X, Wu Y, Jin S, Tian Y, Zhang X, Zhao Y, et al. Gold Nanoparticles Induce Autophagosome Accumulation through Size-Dependent Nanoparticle Uptake and Lysosome Impairment. ACS Nano. 2011; 5: 8629-39.
47. Zhang J, Zhang X, Liu G, Chang D, Liang X, Zhu X, et al. Intracellular Trafficking Network of Protein Nanocapsules: Endocytosis, Exocytosis and Autophagy. Theranostics. 2016; 6: 2099-2113.